



PERGAMON

International Journal of Solids and Structures 38 (2001) 1395–1414

INTERNATIONAL JOURNAL OF
**SOLIDS and
STRUCTURES**

www.elsevier.com/locate/ijsostr

Generalized plane strain thermoelastic deformation of laminated anisotropic thick plates

Senthil S. Vel *, R.C. Batra

Department of Engineering Science and Mechanics, Virginia Polytechnic Institute and State University, Blacksburg, VA 24061-0219, USA

Received 3 September 1999; in revised form 22 February 2000

Abstract

The generalized plane strain quasi-static thermoelastic deformations of laminated anisotropic thick plates are analyzed by using the Eshelby–Stroh formalism. The laminated plate consists of homogeneous laminae of arbitrary thicknesses. The three-dimensional equations of linear anisotropic thermoelasticity simplified to the case of generalized plane strain deformations are exactly satisfied at every point in the body. The analytical solution is in terms of an infinite series; the continuity conditions at the interfaces and boundary conditions at the bounding surfaces are used to determine the coefficients. The formulation admits different mechanical and thermal boundary conditions at the edges of each lamina, and is applicable to thick and thin laminated plates. Results are computed for thick laminated plates with edges either rigidly clamped, simply supported or traction-free and compared with the predictions of the classical laminated plate theory and the first-order shear deformation theory. The boundary layer effect near clamped and traction-free edges is investigated. © 2001 Elsevier Science Ltd. All rights reserved.

Keywords: Analytical solution; Cylindrical bending; Eshelby–Stroh formalism; Thermal stresses

1. Introduction

Advanced composite materials offer numerous superior properties like high strength-to-weight ratio and nearly zero coefficient of thermal expansion in the fiber direction. Their strength and stiffness can be tailored to meet stringent design requirements for high-speed aircrafts, spacecrafts and space structures. This has resulted in their extensive use in structures that are subjected to severe variations in temperature. Thermal stresses, especially at the interface between two different materials, often represent a significant factor in the failure of laminated composite structures. Thus, there is a need to accurately predict thermal stresses in composite structures.

Thermal bending of homogeneous anisotropic thin plates has been investigated by Pell (1946). Subsequently, Stavsky (1963) studied the thermal deformation of laminated anisotropic plates. These early

* Corresponding author.

E-mail address: senthil@vt.edu (S.S. Vel).

studies employed the classical laminated plate theory (CLPT) that is based on the Kirchhoff–Love hypothesis. Wu and Tauchert (1980a,b) used the CLPT to study the thermal deformation of laminated rectangular plates. The CLPT neglects transverse shear deformation and can lead to significant errors for moderately thick plates. Yang et al. (1966) and Whitney and Pagano (1970) developed the first-order shear deformation theory (FSDT) for laminated elastic plates. It extends the kinematics of the CLPT by incorporating transverse shear strains that are constant through the thickness of the laminate. Reddy et al. (1980) and Reddy and Hsu (1980) extended the FSDT for thermal deformation and stresses. Various higher-order theories for the thermal analysis of laminated plates have been reported by Cho et al. (1989), Khdeir and Reddy (1991, 1999) and Murakami (1993). We refer the reader to Tauchert (1991), Noor and Burton (1992), Jones (1975) and Reddy (1997) for a historical perspective and for a review of various approximate theories.

The validity of approximate plate theories and finite-element solutions can be assessed by comparing their predictions with the analytical solutions of the three-dimensional equations of anisotropic thermoelasticity (Noor et al., 1994; Murakami, 1993; Ali et al., 1999). Srinivas and Rao (1972) obtained a three-dimensional solution for the flexure of laminated, isotropic, simply supported plates. Tauchert (1980) gave exact thermoelasticity solutions to the plane-strain deformation of orthotropic simply supported laminates using the method of displacement potentials. Thangjitham and Choi (1991) gave an exact solution for laminated infinite plates using the Fourier transform technique and the stiffness matrix method. Murakami (1993) generalized the work of Pagano (1970) to the cylindrical bending of simply supported laminates subjected to thermal loads. Tungikar and Rao (1994), Noor et al. (1994) and Savoia and Reddy (1995, 1997) gave exact three-dimensional solutions for thermal stresses in simply supported anisotropic rectangular laminates. However, simply supported edge conditions are less often realized in practice, and they do not exhibit a well-known boundary layer/edge effects near clamped and traction-free edges. The accuracy of plate theories near and within the edge layer are yet to be carefully investigated.

The Eshelby–Stroh formalism (Eshelby et al., 1953; Stroh, 1958; Ting, 1996) provides exact solutions to the governing equations of anisotropic elasticity under generalized plane-strain deformations in terms of analytic functions. Recently, Vel and Batra (1999, 2000) adopted a series solution for the analytic functions to study the generalized plane-strain and three-dimensional deformations of laminated elastic plates subjected to arbitrary boundary conditions. Here, the method is extended to thermoelastic problems. The mechanical equilibrium and steady-state heat conduction equations are exactly satisfied, and various constants in the general solution are determined from the boundary conditions at the bounding surfaces and continuity conditions at the interfaces between adjoining laminae. This results in an infinite system of linear equations in infinitely many unknowns. By retaining a large number of terms in the series, the solution can be computed to any desired degree of accuracy. The formulation admits different mechanical and thermal boundary conditions at the edges of each lamina and is applicable to thick and thin laminated plates. The procedure is illustrated by computing results for the cylindrical bending of thick laminated plates with edges either rigidly clamped, simply supported or traction-free and comparing them with the predictions of the CLPT and the FSDT.

2. Problem formulation

We use a rectangular Cartesian coordinate system, shown in Fig. 1, to describe the infinitesimal quasi-static thermoelastic deformations of an N -layer laminated elastic plate occupying the region $[0, L_1] \times (-\infty, \infty) \times [0, L_3]$ in the unstressed reference configuration. Here, x_1 and x_2 are the in-plane coordinates and x_3 , the thickness coordinate of the plate. Planes $x_3 = L_3^{(1)}, L_3^{(2)}, \dots, L_3^{(n)}, \dots, L_3^{(N+1)}$ describe, respectively, the lower bounding surface, the interface between the bottom-most and the adjoining lamina, the interfaces between abutting laminae, and the top bounding surface.

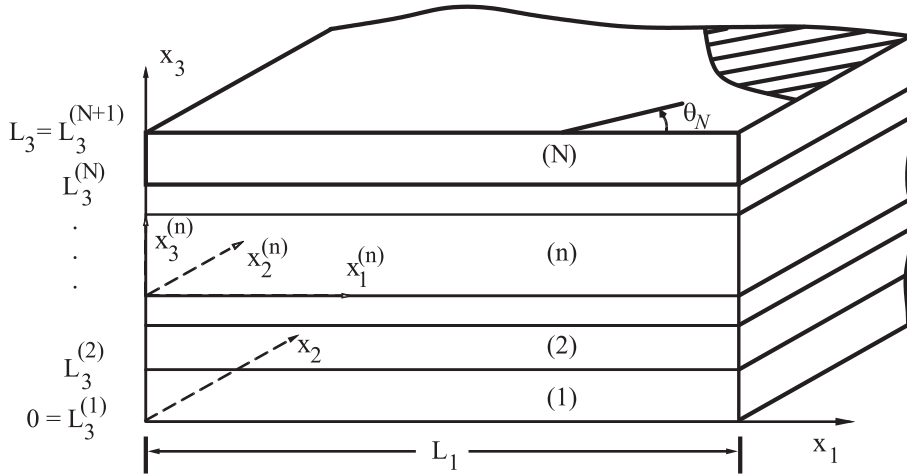


Fig. 1. An N -layer laminated thick plate.

The equations of mechanical and thermal equilibrium in the absence of body forces and internal heat sources are (Carlson, 1972)

$$\sigma_{jm,m} = 0, \quad q_{m,m} = 0 \quad (j, m = 1-3), \tag{1a, b}$$

where σ_{jm} are the components of the Cauchy stress tensor and q_m , the heat flux. A comma followed by index m denotes partial differentiation with respect to the present position x_m of a material particle, and a repeated index implies summation over the range of the index.

The constitutive equations for a linear anisotropic thermoelastic material are (Carlson, 1972)

$$\sigma_{jm} = C_{jmqr} \varepsilon_{qr} - \beta_{jm} T, \quad q_m = -\kappa_{mr} T_{,r}, \tag{2a, b}$$

where C_{jmqr} are the components of the elasticity tensor, ε_{qr} , the infinitesimal strain tensor, β_{jm} , the thermal stress moduli, T , the change in temperature of the material particle from that in the stress-free reference configuration and κ_{mr} , the thermal conductivity tensor. The infinitesimal strain tensor is related to the mechanical displacements u_q by

$$\varepsilon_{qr} = \frac{1}{2}(u_{q,r} + u_{r,q}).$$

The mechanical and thermal equations are uncoupled in the sense that the temperature field can first be determined by solving Eqs. (1b) and (2b), and displacements \mathbf{u} can then be found from Eqs. (1a) and (2a). Material elasticities are assumed to exhibit the symmetries $C_{jmqr} = C_{mjqr} = C_{qjrm}$. Furthermore, the elasticity tensor and the thermal conductivity tensor are assumed to be positive definite.

The displacement and/or traction components prescribed on the edges $x_1 = 0$ and L_1 , and bottom and top surfaces $x_3 = 0$ and L_3 are presumed not to depend upon x_2 , and are specified as follows (Ting, 1996, pp. 497–498):

$$\begin{aligned} \mathbf{I}_u^{(s)} \mathbf{u} + \mathbf{I}_\sigma^{(s)} \boldsymbol{\sigma}_s &= \boldsymbol{\vartheta}^{(s)} \quad \text{on } x_s = 0, \\ \tilde{\mathbf{I}}_u^{(s)} \mathbf{u} + \tilde{\mathbf{I}}_\sigma^{(s)} \boldsymbol{\sigma}_s &= \tilde{\boldsymbol{\vartheta}}^{(s)} \quad \text{on } x_s = L_s \quad (s = 1, 3), \end{aligned} \tag{3}$$

where $(\boldsymbol{\sigma}_s)_k = \sigma_{ks}$ and $\mathbf{I}_u^{(s)}, \mathbf{I}_\sigma^{(s)}, \tilde{\mathbf{I}}_u^{(s)}$ and $\tilde{\mathbf{I}}_\sigma^{(s)}$ are 3×3 diagonal matrices, while $\boldsymbol{\vartheta}^{(s)}$ and $\tilde{\boldsymbol{\vartheta}}^{(s)}$ are known vector functions. For ideal restraints at the edges, these diagonal matrices have entries of either zero or one such that

$$\mathbf{I}_u^{(s)} + \mathbf{I}_\sigma^{(s)} = \tilde{\mathbf{I}}_u^{(s)} + \tilde{\mathbf{I}}_\sigma^{(s)} = \mathbf{I} \quad (s = 1) \quad (4)$$

with \mathbf{I} being the 3×3 identity matrix. In other words, we specify on the boundary either a component of the displacement or traction vector in each coordinate direction. For ideal restraints at the edges, if the surface $x_1 = 0$ is rigidly clamped (C), then $\mathbf{I}_u^{(1)} = \mathbf{I}$, $\mathbf{I}_\sigma^{(1)} = \mathbf{0}$ and $\boldsymbol{\vartheta}^{(1)} = \mathbf{0}$, i.e. $u_1 = u_2 = u_3 = \mathbf{0}$. Boundary conditions for traction-free (F) and simply supported (S) edges may be specified by $\mathbf{I}_u^{(1)} = \mathbf{0}$, $\mathbf{I}_\sigma^{(1)} = \mathbf{I}$, $\boldsymbol{\vartheta}^{(1)} = \mathbf{0}$ and $\mathbf{I}_u^{(1)} = \text{diag}[0, 0, 1]$, $\mathbf{I}_\sigma^{(1)} = \text{diag}[1, 1, 0]$, $\boldsymbol{\vartheta}^{(1)} = \mathbf{0}$, respectively. The specification of the boundary conditions at a simply supported edge, namely $\sigma_{11} = \sigma_{12} = 0$, $u_3 = 0$, is identical to that used by Pagano (1970). The method is also applicable when the edges are elastically restrained or when the laminate is on an elastic foundation in which case the diagonal matrices need not satisfy Eq. (4). The thermal boundary conditions are specified as

$$\begin{aligned} m^{(s)}T + r^{(s)}q_s &= \varphi^{(s)} \quad \text{on } x_s = 0, \\ \tilde{m}^{(s)}T + \tilde{r}^{(s)}q_s &= \tilde{\varphi}^{(s)} \quad \text{on } x_s = L_s \quad (s = 1, 3). \end{aligned} \quad (5a, b)$$

By appropriately choosing $m^{(s)}$, $r^{(s)}$, $\tilde{m}^{(s)}$ and $\tilde{r}^{(s)}$ in these equations, various thermal boundary conditions corresponding to the prescribed temperature, prescribed heat flux and exposure to an ambient temperature through a boundary conductance can be specified. The interfaces between adjoining laminae are assumed to be perfectly bonded together and in ideal thermal contact, so that

$$[[\mathbf{u}]] = 0, \quad [[\boldsymbol{\sigma}_3]] = 0, \quad [[T]] = 0, \quad [[q_3]] = 0 \quad \text{on } x_3 = L_3^{(2)}, L_3^{(3)}, \dots, L_3^{(N)}. \quad (6a, b, c, d)$$

Here, $[[\mathbf{u}]]$ denotes the jump in the value of \mathbf{u} across an interface.

Since the applied loads are independent of x_2 , the body is of infinite extent in the x_2 direction, and material properties are uniform, we postulate that the displacement \mathbf{u} and temperature T are functions of x_1 and x_3 only, and thus correspond to generalized plane deformation.

3. Thermoelasticity solution

The Eshelby–Stroh formalism (Eshelby et al., 1953; Stroh, 1958; Ting, 1996) provides a general solution for the generalized plane-strain deformation of an anisotropic elastic body. It was extended to anisotropic thermoelasticity by Clements (1973), Wu (1984) and Hwu (1990). The general solution satisfies the governing Eqs. (1a), (1b), (2a) and (2b) exactly and is in terms of arbitrary analytic functions. We assume an infinite series expansion for each analytic function. Boundary conditions (3) and (5), and interface conditions (6) are used to determine the coefficients in the series expansion. We construct a local coordinate system $x_1^{(n)}, x_2^{(n)}, x_3^{(n)}$ with origin at the point where the global x_3 axis intersects the bottom surface of the n th lamina; the local axes are parallel to the global axes (Fig. 1). The thickness of the n th lamina is denoted by $h^{(n)} = L_3^{(n+1)} - L_3^{(n)}$.

3.1. A general solution

In deriving a general solution of Eqs. (1a), (1b), (2a) and (2b) for the n th lamina, we drop the superscript n for convenience, it being understood that all material properties and variables belong to this lamina. Assume that

$$\mathbf{u} = \mathbf{a}f(z) + \mathbf{c}g(z_\tau), \quad T = g'(z_\tau), \quad (7)$$

where

$$z = x_1 + px_3, \quad z_\tau = x_1 + \tau x_3,$$

f and g are arbitrary analytic functions of their arguments, \mathbf{a} , \mathbf{c} , p and τ are possible complex constants to be determined, and $g'(z_\tau) = dg/dz_\tau$. Substitution from Eq. (7) into Eq. (2) and the result into Eq. (1) gives (Ting, 1996)

$$\begin{aligned} \mathbf{D}(p)\mathbf{a} &= \mathbf{0}, \\ \mathbf{D}(\tau)\mathbf{c} &= \boldsymbol{\beta}_1 + \tau\boldsymbol{\beta}_3, \\ \kappa_{33}\tau^2 + (\kappa_{13} + \kappa_{31})\tau + \kappa_{11} &= 0, \end{aligned} \tag{8a, b, c}$$

where

$$\begin{aligned} \mathbf{D}(p) &= \mathbf{Q} + p(\mathbf{R} + \mathbf{R}^T) + p^2\mathbf{T}, \quad Q_{ik} = C_{i1k1}, \quad R_{ik} = C_{i1k3}, \\ T_{ik} &= C_{i3k3}, \quad (\boldsymbol{\beta}_k)_i = \beta_{ik} \quad (i, k = 1-3). \end{aligned}$$

The eigenvalue τ depends on the components of the heat conduction tensor and satisfies the quadratic equations (8c). Since κ_{ij} is positive definite, τ obtained by solving Eq. (8c) cannot be real (Clements, 1973; Ting, 1996). We denote the root with positive imaginary part by τ and its complex conjugate by $\bar{\tau}$. The eigenvalues p and their associated eigenvectors \mathbf{a} are obtained by solving the eigenvalue problem (8a). Since C_{jmqr} is a positive definite tensor, p cannot be real (Eshelby et al., 1953; Ting, 1996). Therefore, there are three pairs of complex conjugates for p . Let

$$\text{Im}(p_\alpha) > 0, \quad p_{\alpha+3} = \bar{p}_\alpha, \quad \mathbf{a}_{\alpha+3} = \bar{\mathbf{a}}_\alpha \quad (\alpha = 1-3). \tag{9a, b, c}$$

The vector \mathbf{c} associated with the thermal eigenvalue τ is obtained by solving the system of equations (8b). If the eigenvalues p_α and τ are distinct, a general solution of Eqs. (1) and (2) obtained by superposing solutions of the form (7) is

$$\begin{aligned} \mathbf{u} &= \sum_{\alpha=1}^3 [\mathbf{a}_\alpha f_\alpha(z_\alpha) + \bar{\mathbf{a}}_\alpha f_{\alpha+3}(\bar{z}_\alpha)] + \mathbf{c} g_1(z_\tau) + \bar{\mathbf{c}} g_2(\bar{z}_\tau), \\ T &= g'_1(z_\tau) + g'_2(\bar{z}_\tau), \end{aligned} \tag{10}$$

where f_α ($\alpha = 1, 2, \dots, 6$), g_1 and g_2 are arbitrary analytic functions, and $z_\alpha = x_1 + p_\alpha x_3$. Substitution of Eq. (10) into Eq. (2) gives

$$\begin{aligned} \boldsymbol{\sigma}_1 &= \sum_{\alpha=1}^3 [-p_\alpha \mathbf{b}_\alpha f'_\alpha(z_\alpha) - \bar{p}_\alpha \bar{\mathbf{b}}_\alpha f'_{\alpha+3}(\bar{z}_\alpha)] - \tau \mathbf{d} g'_1(z_\tau) - \bar{\tau} \bar{\mathbf{d}} g'_2(\bar{z}_\tau), \\ \boldsymbol{\sigma}_3 &= \sum_{\alpha=1}^3 [\mathbf{b}_\alpha f'_\alpha(z_\alpha) + \bar{\mathbf{b}}_\alpha f'_{\alpha+3}(\bar{z}_\alpha)] + \mathbf{d} g'_1(z_\tau) + \bar{\mathbf{d}} g'_2(\bar{z}_\tau), \\ \mathbf{q} &= -(\boldsymbol{\kappa}_1 + \tau \boldsymbol{\kappa}_3) g''_1(z_\tau) - (\boldsymbol{\kappa}_1 + \bar{\tau} \boldsymbol{\kappa}_3) g''_2(\bar{z}_\tau), \end{aligned} \tag{11}$$

where

$$\mathbf{b}_\alpha = (\mathbf{R}^T + p_\alpha \mathbf{T}) \mathbf{a}_\alpha, \quad \mathbf{d} = (\mathbf{R}^T + \tau \mathbf{T}) \mathbf{c} - \boldsymbol{\beta}_3, \quad (\boldsymbol{\kappa}_m)_j = \kappa_{jm}.$$

The general solution (10) and (11) is also applicable when (a) there exist three independent eigenvectors \mathbf{a}_α even when the eigenvalues p_α ($\alpha = 1-3$) are not distinct, and (b) either τ is not equal to one of the p 's or, if $\tau = p$, then Eq. (8b) can be solved for \mathbf{c} . Anisotropic materials that do not satisfy these conditions are called *degenerate thermoelastic materials*. Isotropic materials are a special group of degenerate materials for which $p_\alpha = \tau = i$. Wu (1984) and Yang et al. (1997) have described how the general solution for degenerate materials can be constructed. Consider a degenerate material for which $p_1 = p_2 \neq p_3$, $\tau \neq p_\alpha$ and there is only one eigenvector \mathbf{a}_1 associated with the double root p_1 . A second independent solution associated with the eigenvalue p_1 is

$$\mathbf{u} = \frac{d}{dp_1} [\mathbf{a}_1 f_2(z_1)] = \frac{d\mathbf{a}_1}{dp_1} f_2(z_1) + \mathbf{a}_1 \frac{df_2(z_1)}{dp_1}. \tag{12}$$

Here, $d\mathbf{a}_1/dp_1$ is obtained by differentiating Eq. (8a):

$$\mathbf{D} \frac{d\mathbf{a}_1}{dp_1} + \frac{d\mathbf{D}}{dp_1} \mathbf{a}_1 = \mathbf{0}. \tag{13}$$

Dempsey and Sinclair (1979) have proved the existence of a non-trivial solution for \mathbf{a}_1 and $d\mathbf{a}_1/dp_1$ of Eqs. (8a) and (13). Therefore, the general solution is

$$\begin{aligned} \mathbf{u} &= \sum_{\alpha=1}^3 [\mathbf{a}_\alpha f_\alpha(z_\alpha) + \bar{\mathbf{a}}_\alpha f_{\alpha+3}(\bar{z}_\alpha)] + \mathbf{a}_1 \frac{df_2(z_1)}{dp_1} + \bar{\mathbf{a}}_1 \frac{df_5(\bar{z}_1)}{d\bar{p}_1} + \mathbf{c} g_1(z_\tau) + \bar{\mathbf{c}} g_2(\bar{z}_\tau), \\ T &= g'_1(z_\tau) + g'_2(\bar{z}_\tau), \end{aligned} \tag{14}$$

where $\mathbf{a}_2 = d\mathbf{a}_1/dp_1$. The corresponding general solution for the stress tensor and the heat flux is obtained by substituting Eq. (14) into Eq. (2). It is important to note that, irrespective of whether the material is degenerate or not, there are eight arbitrary analytic functions, namely f_α ($\alpha = 1, 2, \dots, 6$), g_1 and g_2 . Our treatment of the degenerate case differs from that of Wu (1984) and Yang et al. (1997) only in one aspect, namely, we do not require $f_2(z_1) = f_1(z_1)$ as they do.

3.2. A series solution

Even though Eq. (10) satisfies Eq. (1) for all choices of the analytic functions f_α , g_1 and g_2 , a choice based on the geometry of the problem and boundary conditions can reduce the algebraic work involved. We select for the n th lamina

$$\begin{aligned} f_\alpha(z_\alpha) &= \sum_{m=0}^{\infty} \{v_{m\alpha}^{(1)} \exp(\eta_{m\alpha} z_\alpha) + w_{m\alpha}^{(1)} \exp(\eta_{m\alpha} (l - z_\alpha))\} + \sum_{k=0}^{\infty} \{v_{k\alpha}^{(3)} \exp(\lambda_{k\alpha} z_\alpha) \\ &\quad + w_{k\alpha}^{(3)} \exp(\lambda_{k\alpha} (p_\alpha h - z_\alpha))\}, \\ f_{\alpha+3}(\bar{z}_\alpha) &= \overline{f_\alpha(z_\alpha)} \quad (\alpha = 1-3), \end{aligned} \tag{15a, b}$$

where $0 \leq x_1 \leq l$, $0 \leq x_3 \leq h$,

$$\eta_{m\alpha} = \begin{cases} -\frac{m_0 \pi i}{p_\alpha h} & \text{if } m = 0 \\ -\frac{m \pi i}{p_\alpha h} & \text{if } m \geq 1 \end{cases}, \quad \lambda_{k\alpha} = \begin{cases} \frac{k_0 \pi i}{l} & \text{if } k = 0 \\ \frac{k \pi i}{l} & \text{if } k \geq 1 \end{cases}, \tag{16}$$

$i = \sqrt{-1}$ and $m_0, k_0 \in (0, 1)$. The functions g_1 and g_2 are chosen as

$$\begin{aligned} g_1(z_\tau) &= \sum_{m=0}^{\infty} \{\hat{v}_m^{(1)} \exp(\zeta_m z_\tau) + \hat{w}_m^{(1)} \exp(\zeta_m (l - z_\tau))\} + \sum_{k=0}^{\infty} \{\hat{v}_k^{(3)} \exp(\zeta_k z_\tau) \\ &\quad + \hat{w}_k^{(3)} \exp(\zeta_k (\tau h - z_\tau))\}, \\ g_2(\bar{z}_\tau) &= \overline{g_1(z_\tau)}, \end{aligned} \tag{17a, b}$$

where $z_\tau = x_1 + \tau x_3$ and

$$\zeta_m = \begin{cases} -\frac{m_0 \pi i}{\tau h} & \text{if } m = 0 \\ -\frac{m \pi i}{\tau h} & \text{if } m \geq 1 \end{cases}, \quad \zeta_k = \begin{cases} \frac{k_0 \pi i}{l} & \text{if } k = 0 \\ \frac{k \pi i}{l} & \text{if } k \geq 1 \end{cases}. \tag{18}$$

The function $\exp(\eta_{m\alpha} z_\alpha)$ in Eq. (15) varies sinusoidally on the surface $x_1 = 0$ of the n th lamina and decays exponentially in the x_1 direction. With increasing k , higher harmonics are introduced on the surface $x_1 = 0$

accompanied by steeper exponential decay in the x_1 direction. Similarly, functions $\exp(\eta_{m\alpha}(l - z_\alpha))$, $\exp(\lambda_{k\alpha}z_\alpha)$ and $\exp(\lambda_{k\alpha}(p_\alpha h - z_\alpha))$ vary sinusoidally on surfaces $x_1 = l$, $x_3 = 0$ and $x_3 = h$, respectively. In essence, single Fourier series in the x_1 and x_3 directions are superposed for each lamina to solve the problem. This idea of superposing single Fourier series dates back to Mathieu (1890), who used it to analyze the plane strain deformation of a rectangular region of isotropic material subjected to arbitrary tractions on the boundaries. The inequality in (9a) ensures that all functions decay exponentially towards the interior of the lamina. The choices (15b) and (17b) for $f_{\alpha+3}(\bar{z}_\alpha)$ and $g_2(\bar{z}_\tau)$ ensure that the mechanical displacements, stresses, temperature change and heat flux are real valued. The functions involving m_0 and k_0 play the role of a constant term in the Fourier series expansion.

The unknowns $\mathbf{v}_{k\alpha}^{(s)}$, $\mathbf{w}_{k\alpha}^{(s)}$, $\hat{\mathbf{v}}_k^{(s)}$, $\hat{\mathbf{w}}_k^{(s)}$ ($s = 1, 3$) are assumed to be complex for $k \neq 0$ and real when $k = 0$. The superscript s indicates that the exponential function associated with the unknown has a sinusoidal variation on the surface $x_s = \text{constant}$. Substitution of Eqs. (15a), (15b), (17a) and (17b) into the general solution (10) and (11) results in the following expressions for the displacements and the temperature change for nondegenerate materials:

$$\begin{aligned} \mathbf{u} = & \mathbf{A} \left\{ \sum_{m=0}^{\infty} [\langle \exp(\eta_{m*} z_*) \rangle \mathbf{v}_m^{(1)} + \langle \exp(\eta_{m*}(l - z_*)) \rangle \mathbf{w}_m^{(1)}] \right. \\ & \left. + \sum_{k=0}^{\infty} [\langle \exp(\lambda_{k*} z_*) \rangle \mathbf{v}_k^{(3)} + \langle \exp(\lambda_{k*}(p_* h - z_*)) \rangle \mathbf{w}_k^{(3)}] \right\} \\ & + \mathbf{c} \left\{ \sum_{m=0}^{\infty} [\exp(\zeta_m z_\tau) \hat{\mathbf{v}}_m^{(1)} + \exp(\zeta_m(l - z_\tau)) \hat{\mathbf{w}}_m^{(1)}] \right. \\ & \left. + \sum_{k=0}^{\infty} [\exp(\zeta_k z_\tau) \hat{\mathbf{v}}_k^{(3)} + \exp(\zeta_k(\tau h - z_\tau)) \hat{\mathbf{w}}_k^{(3)}] \right\} + \text{conjugate}, \tag{19a, b} \\ T = & \sum_{m=0}^{\infty} [\zeta_m \exp(\zeta_m z_\tau) \hat{\mathbf{v}}_m^{(1)} - \zeta_m \exp(\zeta_m(l - z_\tau)) \hat{\mathbf{w}}_m^{(1)}] \\ & + \sum_{k=0}^{\infty} [\zeta_k \exp(\zeta_k z_\tau) \hat{\mathbf{v}}_k^{(3)} - \zeta_k \exp(\zeta_k(\tau h - z_\tau)) \hat{\mathbf{w}}_k^{(3)}] + \text{conjugate}, \end{aligned}$$

where

$$\begin{aligned} \mathbf{A} = & [\mathbf{a}_1, \mathbf{a}_2, \mathbf{a}_3], \quad \langle \psi(z_*) \rangle = \text{diag}[\psi(z_1), \psi(z_2), \psi(z_3)], \\ (\mathbf{v}_m^{(s)})_\alpha = & \mathbf{v}_{m\alpha}^{(s)}, \quad (\mathbf{w}_m^{(s)})_\alpha = \mathbf{w}_{m\alpha}^{(s)}, \quad \alpha = 1-3, \end{aligned}$$

and conjugate stands for the complex conjugate of the explicitly stated terms. Expressions for stresses and heat flux are derived by substituting from Eq. (19) into Eq. (2). Our choice of analytic functions remains the same for a degenerate material, and the corresponding expressions for the displacement and the temperature change are obtained by substituting them into the appropriately modified general solution. As an example, for the degeneracy considered earlier, the expressions for the displacements and the temperature are obtained by substituting Eqs. (15) and (17) into Eq. (14).

3.3. Satisfaction of boundary and interface conditions

Each lamina has its own set of unknowns $\mathbf{v}_k^{(s)}$, $\mathbf{w}_k^{(s)}$, $\hat{\mathbf{v}}_k^{(s)}$, $\hat{\mathbf{w}}_k^{(s)}$ ($s = 1, 3$). These are determined from the interface continuity conditions and boundary conditions on all surfaces of the laminate by the classical Fourier series method.

Since the heat conduction problem is uncoupled from the mechanical problem, we first determine the temperature field by imposing the thermal boundary conditions on the four bounding surfaces of the laminate and the continuity of temperature and heat flux across the interfaces between the adjoining laminae. On the top surface $x_3^{(N)} = L_3^{(N+1)}$ of the laminate, we extend the component functions defined over $(0, L_1)$ in Eq. (19b) to the interval $(-L_1, 0)$ in the x_1 direction. The functions $\exp(\zeta_k z_\tau)$ and $\exp(\zeta_k(\tau h - z_\tau))$ that are sinusoidal in the x_1 direction are extended without modification since they form the basis functions on this surface, except for $\exp(\zeta_0 z_\tau)$ and $\exp(\zeta_0(\tau h - z_\tau))$ that are extended as even functions since they represent the constant terms in the Fourier series representation. The functions $\exp(\zeta_m z_\tau)$ and $\exp(\zeta_m(l - z_\tau))$ are extended as even functions since they vary exponentially in the x_1 direction. We multiply Eq. (5b) for $s = 3$ by $\exp(j\pi x_1/L_1)$ and integrate the result with respect to x_1 from $-L_1$ to L_1 to obtain

$$\int_{-L_1}^{L_1} \{ \tilde{m}^{(3)} T + \tilde{r}^{(3)} q_3 - \tilde{\varphi}^{(3)} \} \exp(j\pi x_1/L_1) dx_1 = 0 \quad (x_3 = L_3; j = 1, 2, 3, \dots). \quad (20)$$

The same procedure is used to enforce the thermal boundary conditions (5a) and (5b) for the bottom surface, the edges and the interface thermal continuity conditions (6c) and (6d). Substitution of T and \mathbf{q} into Eq. (20) and the other equations that enforce the thermal boundary and interface continuity conditions results in a nonstandard infinite set of linear equations for the unknowns $\hat{v}_k^{(s)}, \hat{w}_k^{(s)}$ ($s = 1, 3$).

The mechanical boundary conditions (3) and interface continuity conditions (6a) and (6b) for the displacement and traction are also enforced in a similar manner. For example, the mechanical boundary conditions on the surface $x_3 = L_3$ will give

$$\int_{-L_1}^{L_1} \{ \tilde{\mathbf{I}}_u^{(3)} \mathbf{u} + \tilde{\mathbf{I}}_\sigma^{(3)} \boldsymbol{\sigma}_3 - \tilde{\boldsymbol{\vartheta}}^{(3)} \} \exp(j\pi x_1/L_1) dx_1 = \mathbf{0}, \quad (x_3 = L_3; j = 1, 2, 3, \dots). \quad (21)$$

Enforcing all the mechanical boundary and interface conditions will give another nonstandard infinite set of linear equations for $\mathbf{v}_m^{(s)}, \mathbf{w}_m^{(s)}$. A general theory for the resulting infinite system of equations does not exist. However, reasonably accurate solutions may be obtained by truncating the series involving summations over m and k in Eqs. (15a), (15b), (17a) and (17b) to K_1 and $K_3^{(n)}$ terms, respectively. In general, we try to maintain approximately the same period of the largest harmonic on all interfaces and boundaries by choosing $K_3^{(n)} = \text{Ceil}(K_1 h^{(n)}/L_1)$, where $\text{Ceil}(y)$ gives the smallest integer greater than or equal to y . The truncated set of coefficients $\hat{v}_k^{(s)}, \hat{w}_k^{(s)}$ are determined first by solving the truncated set of linear equations corresponding to the heat conduction problem. The truncated set of coefficients $\mathbf{v}_m^{(s)}, \mathbf{w}_m^{(s)}$ are determined next by solving the truncated system of linear equations obtained by enforcing the mechanical boundary and interface continuity conditions.

The solution (19) indicates that the component functions decrease exponentially from the boundary/interfaces into the interior of the n th lamina. By truncating the series, we have effectively ignored coefficients with suffices greater than a particular value and approximated the coefficients which have small suffices. Due to the rapid decay of component functions associated with large suffices, the truncation of the series will not greatly influence the solution at the interior points. A larger value of K_1 is expected to give a more accurate solution at points close to the boundary and interfaces. Note that the coefficients $\mathbf{v}_k^{(3)}$ and $\mathbf{w}_k^{(3)}$ in the expressions for the stresses are multiplied by λ_{k*} , and $\mathbf{v}_m^{(1)}$ and $\mathbf{w}_m^{(1)}$ are multiplied by η_{m*} . However, the coefficients of these terms in the expressions (19a) for displacements are unity. Since λ_{k*} and η_{m*} increase as the suffices k and m increase, the terms with large suffices are more significant for the stresses than for the displacements. Thus, the stresses will converge more slowly than the displacements. Once the coefficients have been determined by satisfying the boundary and interface conditions, the displacements, stresses, temperature and heat flux for each lamina are obtained from Eq. (19).

4. Solutions from the CLPT and the FSDT

We assume the following unified displacement field:

$$\begin{aligned}
 u_1(x_1, x_3) &= u_1^0(x_1) + x_3 \left[c_0 \frac{du_3^0}{dx_1} + c_1 \phi_1(x_1) \right], \\
 u_2(x_1, x_3) &= u_2^0(x_1) + c_1 x_3 \phi_2(x_1), \\
 u_3(x_1, x_3) &= u_3^0(x_1),
 \end{aligned}
 \tag{22}$$

where $u_\alpha^0(x_1)$ are the displacements of a point on the bottom surface $x_3 = 0$ which was taken as the reference surface. The displacement field of the CLPT is obtained by setting $c_0 = -1, c_1 = 0$ in Eq. (22), and that of the FSDT, also known as the Reissner–Mindlin plate theory, is obtained by taking $c_0 = 0, c_1 = 1$. The functions ϕ_1 and ϕ_2 in the FSDT are the rotations of the normals about the x_2 and x_1 axes, respectively. The infinitesimal strains associated with the displacement field (22) are

$$\begin{aligned}
 \varepsilon_{11} &= \frac{du_1^0}{dx_1} + x_3 \left[c_0 \frac{d^2u_3^0}{dx_1^2} + c_1 \frac{d\phi_1}{dx_1} \right], & 2\varepsilon_{12} &= \frac{du_2^0}{dx_1} + c_1 x_3 \frac{d\phi_2}{dx_1}, \\
 2\varepsilon_{13} &= (1 + c_0) \frac{du_3^0}{dx_1} + c_1 \phi_1, & 2\varepsilon_{23} &= c_1 \phi_2, & \varepsilon_{22} &= 0.
 \end{aligned}
 \tag{23}$$

The in-plane and transverse stresses for the n th lamina are related to the strains by the constitutive relationship:

$$\begin{aligned}
 \begin{Bmatrix} \sigma_{11} \\ \sigma_{22} \\ \sigma_{12} \end{Bmatrix}^{(n)} &= \begin{bmatrix} \bar{Q}_{11} & \bar{Q}_{12} & \bar{Q}_{16} \\ \bar{Q}_{12} & \bar{Q}_{22} & \bar{Q}_{26} \\ \bar{Q}_{16} & \bar{Q}_{26} & \bar{Q}_{66} \end{bmatrix}^{(n)} \left(\begin{Bmatrix} \varepsilon_{11} \\ \varepsilon_{22} \\ 2\varepsilon_{12} \end{Bmatrix} - \begin{Bmatrix} \alpha_{11} \\ \alpha_{22} \\ 2\alpha_{12} \end{Bmatrix}^{(n)} T \right), \\
 \begin{Bmatrix} \sigma_{23} \\ \sigma_{13} \end{Bmatrix}^{(n)} &= \begin{bmatrix} \bar{Q}_{44} & \bar{Q}_{45} \\ \bar{Q}_{45} & \bar{Q}_{55} \end{bmatrix}^{(n)} \begin{Bmatrix} 2\varepsilon_{23} \\ 2\varepsilon_{13} \end{Bmatrix},
 \end{aligned}
 \tag{24}$$

where \bar{Q}_{ij} and α_{ij} are the reduced elastic stiffnesses and thermal expansion coefficients, respectively (Jones, 1975).

The governing equations, obtained by using the principle of virtual work, are

$$\begin{aligned}
 \frac{dN_{11}}{dx_1} &= 0, & \frac{dN_{12}}{dx_1} &= 0, \\
 c_1 \frac{dM_{11}}{dx_1} - c_1 Q_1 &= 0, & c_1 \frac{dM_{12}}{dx_1} - c_1 Q_2 &= 0, \\
 (1 + c_0) \frac{dQ_1}{dx_1} - c_0 \frac{d^2M_{11}}{dx_1^2} + \hat{f}(x_1) &= 0,
 \end{aligned}
 \tag{25}$$

where the resultants are defined by

$$[N_{\alpha\beta}, M_{\alpha\beta}, Q_\alpha] = \int_0^{L_3} [\sigma_{\alpha\beta}, \sigma_{\alpha\beta}x_3, \mathcal{K} \sigma_{\alpha 3}] dx_3 \quad (\alpha, \beta = 1, 2),
 \tag{26}$$

and \hat{f} is the distributed transverse mechanical load per unit length along the span. The parameter \mathcal{K} that appears in the computation of the shear resultants Q_α is called the shear-correction coefficient. Although the shear-correction coefficient depends on the laminate properties and the lamination scheme, we assume that

$\mathcal{K} = 5/6$ which is widely used in the FSDT literature (Whitney and Pagano, 1970). We assume the following boundary conditions for simply supported (S), clamped (C) and traction-free (F) edges:

$$\begin{aligned}
 S: \quad & N_{11} = N_{12} = 0, \quad c_1 M_{11} = c_1 M_{12} = 0, \quad c_0 M_{11} = 0, \quad u_3^0 = 0, \\
 C: \quad & u_1^0 = u_2^0 = u_3^0 = 0, \quad c_1 \phi_1 = c_1 \phi_2 = 0, \quad -c_0 \frac{du_3^0}{dx_1} = 0, \\
 F: \quad & N_{11} = N_{12} = 0, \quad c_1 M_{11} = c_1 M_{12} = 0, \quad c_0 M_{11} = 0, \quad (1 + c_0) Q_1 - c_0 \frac{dM_{11}}{dx_1} = 0.
 \end{aligned} \tag{27}$$

Some of the boundary conditions in Eq. (27) will be identically satisfied depending on our choice of c_0 and c_1 . The equilibrium equations (25) and boundary conditions (27) can be expressed in terms of the displacements and rotations by substituting Eqs. (23) and (24) into Eq. (26) and the result into Eqs. (25) and (27). For the linear problem considered, we obtain a set of coupled linear ordinary differential equations for the displacements and rotations with the associated boundary conditions at $x_1 = 0, L_1$. They are solved by using Mathematica for the displacements and rotations, and hence the stresses.

In the CLPT, the interlaminar shear stresses σ_{13} and σ_{23} are identically zero when computed from the constitutive equation. However, these stresses and the transverse normal stress σ_{33} may be computed by using the equilibrium equation (1a) after the in-plane stresses σ_{11}, σ_{12} and σ_{22} have been determined:

$$\begin{aligned}
 \sigma_{13}(x_1, x_3) &= - \int_0^{x_3} \frac{\partial \sigma_{11}}{\partial x_1}(x_1, \xi) d\xi, \\
 \sigma_{23}(x_1, x_3) &= - \int_0^{x_3} \frac{\partial \sigma_{12}}{\partial x_1}(x_1, \xi) d\xi, \\
 \sigma_{33}(x_1, x_3) &= \sigma_{33}(x_1, 0) - \int_0^{x_3} \frac{\partial \sigma_{13}}{\partial x_1}(x_1, \xi) d\xi,
 \end{aligned} \tag{28}$$

where it is assumed that the shear traction vanishes on the top and bottom surfaces. The transverse stresses thus obtained are continuous across the interfaces between adjoining laminae. The same procedure is employed for the FSDT since the transverse shear stresses obtained from the constitutive equations, although nonzero, may be discontinuous across the interfaces between adjoining laminae.

5. Results and discussion

We consider layers of unidirectional fiber reinforced graphite–epoxy material, model each layer as orthotropic and assign the following values to its mechanical and thermal material parameters:

$$\begin{aligned}
 E_L = E_0, \quad E_T = E_0/10, \quad G_{LT} = E_0/20, \quad G_{TT} = E_0/50, \quad \nu_{LT} = \nu_{TT} = 1/4, \\
 \alpha_L = \alpha_0, \quad \alpha_T = 7.2\alpha_0, \quad \kappa_L = 100\kappa_0, \quad \kappa_T = \kappa_0,
 \end{aligned} \tag{29}$$

where E is the Young's modulus, G , the shear modulus, ν , the Poisson's ratio, α , the coefficient of thermal expansion, κ , the thermal conductivity, and subscripts L and T indicate directions parallel and perpendicular to the fibers, respectively. The material properties are identical to those used by Tauchert (1980). For values given in Eq. (29), the nonzero components of the elasticity matrix C_{ijkl} , thermal stress moduli β_{ij} and heat conduction tensor κ_{ij} are listed in Table 1 for four different orientations of the fiber with respect to the x_1 axis on the x_1 – x_2 plane. The lamination scheme of the laminate is denoted by $[\theta_1/\theta_2/\dots/\theta_N]$, where θ_n is the angle between the fibers and the x_1 axis in the n th lamina (Fig. 1) and all laminae are of equal thicknesses. In this section, we denote the thickness of the plate by $H(=L_3)$.

Table 1
Non-vanishing material properties of the graphite–epoxy lamina

Property	Lamina			
	0°	90°	45°	−45°
C_{1111}/E_0	1.0169	0.1078	0.3481	0.3481
C_{2222}/E_0	0.1078	1.0169	0.3481	0.3481
C_{3333}/E_0	0.1078	0.1078	0.1078	0.1078
C_{1122}/E_0	0.0339	0.0339	0.2481	0.2481
C_{1133}/E_0	0.0339	0.0278	0.0308	0.0308
C_{2233}/E_0	0.0278	0.0339	0.0308	0.0308
C_{2323}/E_0	0.02	0.05	0.0350	0.0350
C_{3131}/E_0	0.05	0.02	0.0350	0.0350
C_{1212}/E_0	0.05	0.02	0.2642	0.2642
C_{1112}/E_0	0	0	0.2273	−0.2273
C_{2212}/E_0	0	0	0.2273	−0.2273
C_{3312}/E_0	0	0	0.0031	−0.0031
C_{2331}/E_0	0	0	0.0150	−0.0150
$\beta_{11}/\alpha_0 E_0$	1.5051	1.0102	1.2576	1.2576
$\beta_{22}/\alpha_0 E_0$	1.0102	1.5051	1.2576	1.2576
$\beta_{12}/\alpha_0 E_0$	0	0	0.2475	−0.2475
$\beta_{33}/\alpha_0 E_0$	1.0102	1.0102	1.0102	1.0102
κ_{11}/κ_0	100.0	1.0	50.5	50.5
κ_{22}/κ_0	1.0	100.0	50.5	50.5
κ_{12}/κ_0	0	0	49.5	−49.5
κ_{33}/κ_0	1.0	1.0	1.0	1.0

The edges $x_1 = 0$ and L_1 are either clamped ($u_1 = u_2 = u_3 = 0$), or traction-free with ($\sigma_{11} = \sigma_{12} = \sigma_{13} = 0$) or simply supported ($\sigma_{11} = \sigma_{12} = 0, u_3 = 0$). The notation C–F denotes a plate that is clamped at $x_1 = 0$ and traction-free at $x_1 = L_1$, i.e. a cantilever laminate. The top surface $x_3 = H$ is subjected to the sinusoidal temperature increase

$$T(x_1, H) = T_0 \sin \frac{\pi x_1}{L_1},$$

while the bottom surface and the two edges are maintained at the reference temperature. Since the temperature field is assumed to be known in the CLPT and the FSDT, we substitute the temperature field (19b) into Eq. (24). The surfaces $x_3 = 0, H$ are traction-free, i.e. $\sigma_3(x_1, 0) = \sigma_3(x_1, H) = \mathbf{0}$. Thus, the stresses in the laminate are solely due to the temperature distribution applied on the top surface. We do not consider mechanical loads here since the deformation induced by them has been studied by Vel and Batra (2000). For a linear problem, the results for combined mechanical and thermal loading can be obtained by superposition of the corresponding results.

The problem of a simply supported laminate studied by Tauchert (1980) was analyzed by the present method with $K_1 = 500$ terms, and the two sets of results for the temperature, displacements and stresses were identical. The effect of truncation of the series on the accuracy of the solution is investigated for a 0° homogeneous C–S plate. Computed results for the displacements and stresses at specific points in the laminate are listed in Table 2 for $L_1/H = 5$. The following nondimensionalization has been used:

$$\begin{aligned} \tilde{u}_j(x_1, x_3) &= u_j(x_1, x_3)/T_0 \alpha_0 L_1, & \tilde{\sigma}_{jk}(x_1, x_3) &= \sigma_{jk}(x_1, x_3)/E_0 \alpha_0 T_0, \\ \tilde{e}(x_1) &= [u_3(x_1, H) - u_3(x_1, 0)]/u_3(x_1, H/2), \end{aligned}$$

where \tilde{e} is the normalized change in the thickness of the plate. The Table 2 shows that the values of the normalized displacements and stresses do not change upto third decimal place when K_1 is increased from

Table 2

Convergence study for a 0° homogeneous graphite–epoxy C–S laminate subjected to thermal load, $L_1/H = 5$

Theory	$10\bar{u}_1$ (L_1, H)	$10\bar{u}_3$ ($L_1/2, H/2$)	$10\bar{\sigma}_{11}$ ($L_1/2, H$)	$100\bar{\sigma}_{13}$ ($L_1/8, H/2$)	$1000\bar{\sigma}_{33}$ ($L_1/8, H/2$)	$\bar{\epsilon}(L_1/2)$
Analytical						
$K_1 = 50$	2.3771	1.9144	–6.7562	1.5637	–3.1507	1.5059
$K_1 = 100$	2.3884	1.9123	–6.7542	1.5606	–3.1782	1.5076
$K_1 = 200$	2.3927	1.9118	–6.7547	1.5611	–3.1844	1.5080
$K_1 = 400$	2.3942	1.9116	–6.7549	1.5612	–3.1859	1.5081
$K_1 = 500$	2.3945	1.9116	–6.7549	1.5612	–3.1861	1.5081
CLPT	1.8058	1.6080	–7.9608	2.4643	1.4796	–
FSDT	2.1644	2.0563	–7.5999	2.1034	1.4796	–

400 to 500 terms while reasonable accuracy may be obtained with 100 terms. The corresponding CLPT and FSDT solutions are listed for comparison. It should be noted that the present solution with just 50 terms gives substantially better results than those obtained with either the CLPT or the FSDT for stresses and displacements in a thick plate. Whereas the CLPT underpredicts the transverse deflection of the centroid of the laminate by 15.9%, the FSDT overpredicts it by 7.6%. The CLPT and the FSDT overpredict the magnitude of the longitudinal stress σ_{11} by 17.9% and 12.5%, respectively. According to the 3-D theory, the change in the plate thickness at the midspan equals 150.8% of the deflection there. While k_0 and m_0 in Eqs. (16) and (18) were chosen to be 0.5 for this study, a similar convergence behavior was observed for other values of k_0 and m_0 .

Having established the convergence of the thermoelasticity solution, we plot and compare results from the present method with those obtained from the CLPT and the FSDT. The transverse deflection of the midplane of a 0° C–S homogeneous laminate for two different span-to-thickness ratios is depicted in Fig. 2(a) and (b). For $L_1/H = 5$, the CLPT underestimates the magnitude of the midplane deflection and the FSDT overestimates it. The agreement between all three solutions is very good for $L_1/H \geq 20$. For $L_1/H = 5$, the slope at the clamped edge of the deflection curve predicted by the FSDT and the 3-D theory are nonzero; however the two theories give different values of this slope. Fig. 2(c) and (d) show the through-thickness variation of the transverse displacement at the midspan of the plate. While the CLPT and the FSDT yield a constant value for u_3 through the thickness, the thermoelasticity theory predicts a nonlinear distribution. The CLPT and the FSDT underestimate the transverse deflection of the top surface by 66% and 56%, respectively for $L_1/H = 5$. The error reduces to 14% and 12%, respectively for $L_1/H = 20$. If an accurate solution for the transverse displacement is desired, then one should use higher-order plate theories which assume a quadratic or higher-order variation of the transverse displacement through the thickness and take the reference plane other than the midsurface of the plate. Otherwise, a full three-dimensional analysis of the equations of anisotropic thermoelasticity is recommended.

Fig. 3 depicts the longitudinal variation of the transverse shear stress σ_{13} on the midsurface for three different combinations of boundary conditions and for span-to-thickness ratios of 5 and 10. When the edges are simply supported, the percentage error of the CLPT and the FSDT with respect to the thermoelasticity solution remains essentially the same at every point along the span of the plate. The percentage errors near the clamped and traction-free edges of a cantilever plate are significantly larger than those at the midspan, as shown in Fig. 3(c) and (d). This is due to the presence of boundary layers at the clamped and traction-free edges. The width of the boundary layers may be equated with the distance from the edges $x_1 = 0$ or L_1 of the point, where the curvature of the curve σ_{13} vs. x_1 suddenly changes. This definition gives the boundary layer width as approximately $0.25L_1$ and $0.08L_1$ at the clamped and traction-free edges, respectively, for a cantilever plate with span-to-thickness ratio of 5. The boundary layer widths reduce to $0.15L_1$ and $0.04L_1$, respectively when the span-to-thickness ratio equals 10. Thus, the boundary layer width

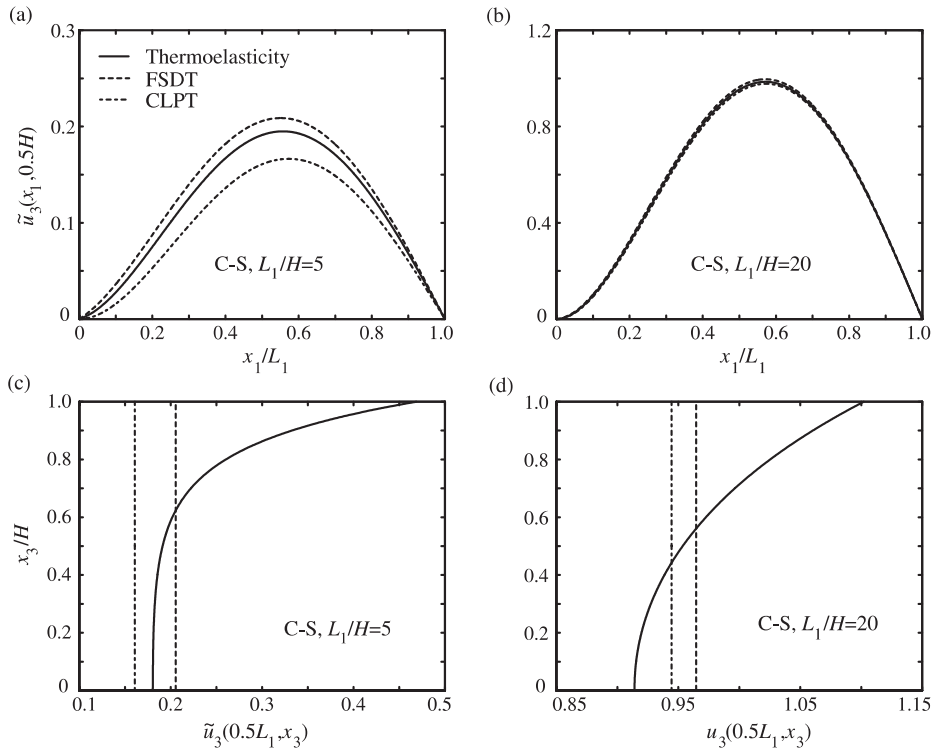


Fig. 2. (a, b) The longitudinal distribution and (c, d) through-thickness distribution of the nondimensional transverse deflection of a clamped-simply supported 0° homogeneous plate for span-to-thickness ratios of 5 and 20. The plate is subjected to a thermal load on the top surface.

strongly depends upon the span-to-thickness ratio of the plate. There is a significant discrepancy between the thermoelasticity solution and the predictions of the CLPT and the FSDT within the boundary layer. The longitudinal variation of the transverse shear stress for a C–S plate is depicted in Fig. 3(e) and (f). Fig. 3(a), (b), (e) and (f) reveal the absence of boundary layers at simply supported edges. The through-thickness variation of the transverse normal stress σ_{33} is shown in Fig. 4 for a C–S plate with the span-to-thickness ratio of 5. As is evident from Fig. 4(a), the CLPT and the FSDT overestimate σ_{33} at the midspan. Fig. 4(b) depicts the through-thickness distribution of σ_{33} at the section $x_1 = 0.1L_1$ which is located near the clamped edge. Although the two plate theories give a tensile transverse normal stress, the thermoelasticity theory predicts it to be compressive.

The through-thickness variation of the longitudinal stress is shown in Fig. 5 for thick ($L_1/H = 5$) cross-ply C–F and C–S laminates. Fiber orientations $[0/90]$ and $[90/0]$ are considered. Fig. 5(a) and (b) evince the through-thickness variation of the longitudinal stress at a section close to the traction-free edge of a cantilever laminate, while Fig. 5(c) and (d) depict corresponding results for a section near the clamped edge of a C–S laminate. The approximate plate theories show good agreement for σ_{11} with the thermoelasticity solution even within the boundary layers at the two edges. The longitudinal stress distribution for cross-ply simply supported laminates are not shown here since they are identical to those given by Tauchert (1980). The transverse shear stress distribution at $x_1 = 0.1L_1$ for thick cross-ply antisymmetric and symmetric C–S laminates is depicted in Fig. 6. Although the FSDT accounts for the transverse shear deformation, its prediction of the transverse shear stress is in considerable error near the clamped edge. The axial variation

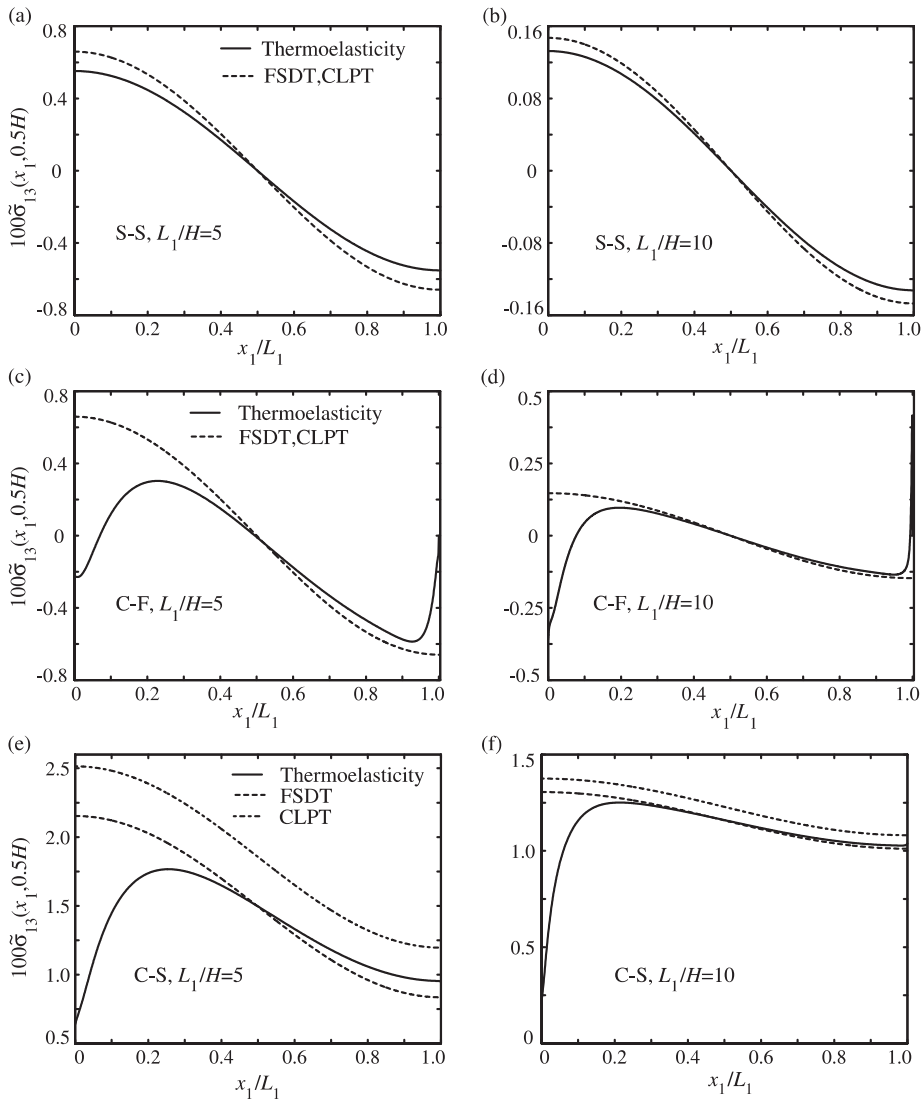


Fig. 3. The longitudinal distribution of the nondimensional transverse shear stress for a 0° homogeneous plate with span-to-thickness ratios of either 5 or 10 and subjected to a thermal load on the top surface: (a, b) simply supported on both edges, (c, d) clamped-free and (e, f) clamped-simply supported.

of the transverse shear stress on the midsurface of antisymmetric and symmetric cross-ply laminates is given in Fig. 7(a) and (b). The midsurface coincides with the interface in the case of the $[0/90]$ laminate. The transverse shear stress in this case exhibits severe oscillations at points on the interface between the 0° lamina and the 90° lamina that are near the clamped edge. This may be due to the presence of a singularity in the stress field at the point $(0, H/2)$ where two right-angle wedges of different materials meet. The existence of a singularity can be confirmed only by performing an asymptotic analysis (Ting and Hwu, 1991). The high-frequency oscillation in the transverse shear stress is associated with component functions involving large values of the index k in the series solution (19a,b). Due to our choice of basis functions in Eqs.

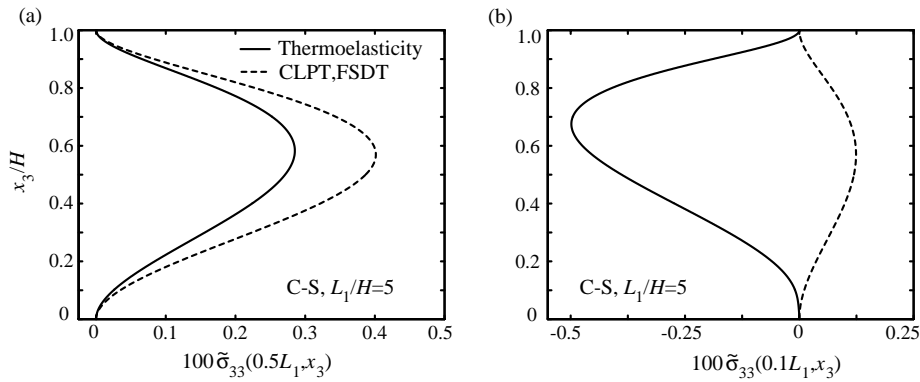


Fig. 4. The through-thickness distribution of the nondimensional transverse normal stress at (a) the midspan and (b) close to the clamped edge of a clamped simply supported 0° homogeneous plate, $L_1/H = 5$, and with a thermal load applied on its top surface.

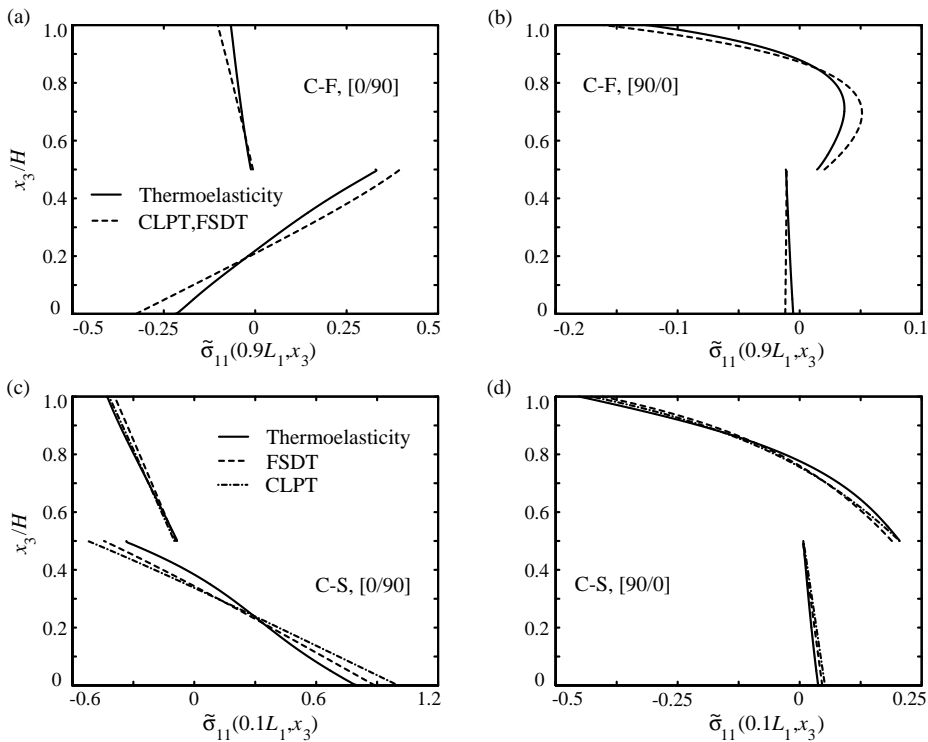


Fig. 5. The through-thickness distribution of the nondimensional longitudinal stress for (a, b) a clamped-free and (c, d) a clamped-simply supported cross-ply laminate, $L_1/H = 5$, and subjected to a thermal load on the top surface.

(15a) and (15b) that exponentially decay towards the interior of each lamina, the high-frequency oscillations decay very rapidly away from the interfaces. In the beam theories, the traction-free boundary conditions at the edge $x_1 = L_1$ are not satisfied pointwise but on the average, i.e., the resultant force there vanishes. In the present thermoelasticity solution, the longitudinal stress vanishes at all points on the

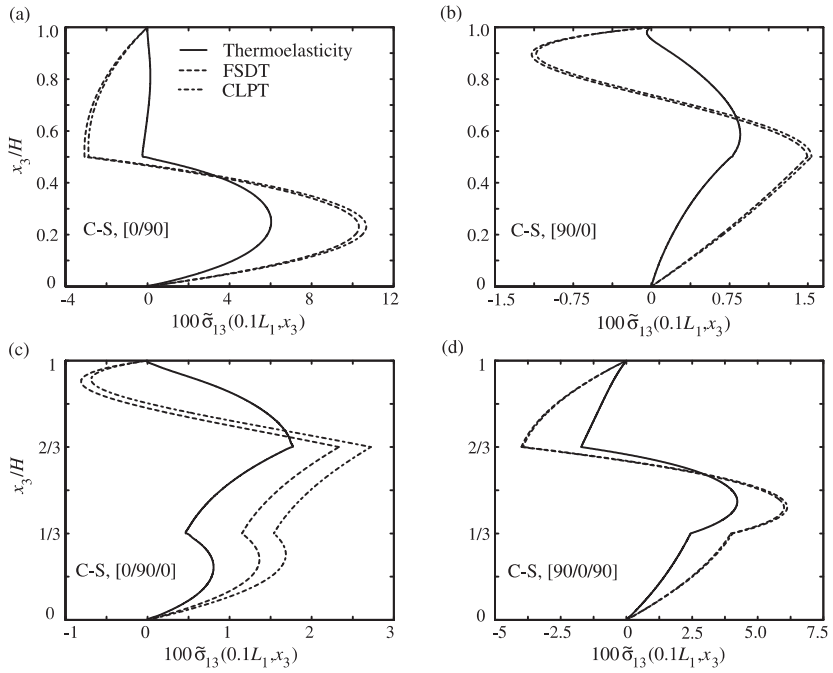


Fig. 6. The through-thickness distribution of the nondimensional transverse shear stress for a clamped-simply supported (a, b) 2-layer and (c, d) 3-layer cross-ply laminates, $L_1/H = 5$. A thermal load is applied on the top surface of the plate.

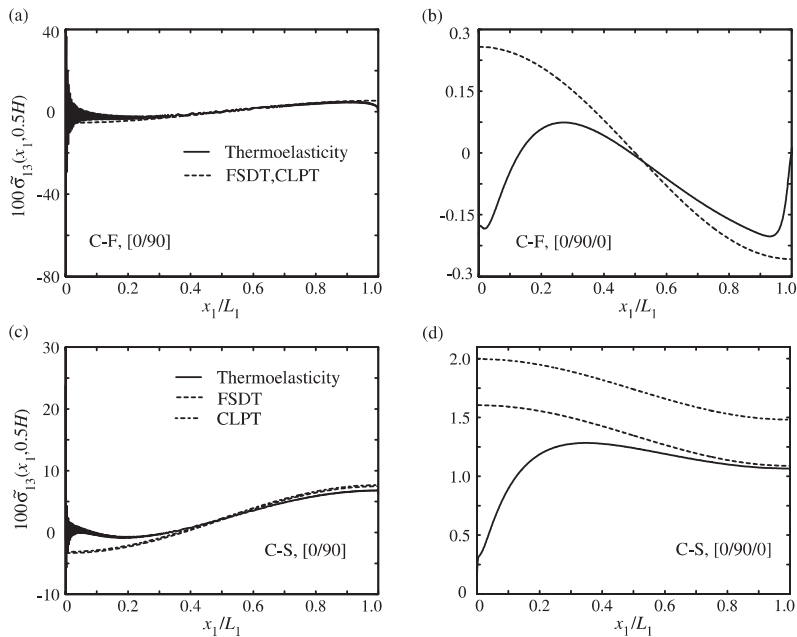


Fig. 7. The longitudinal distribution of the nondimensional transverse shear stress on the midplane of (a, b) a clamped-free and (c, d) a clamped-simply supported cross-ply laminates, $L_1/H = 5$, with a thermal load applied on its top surface.

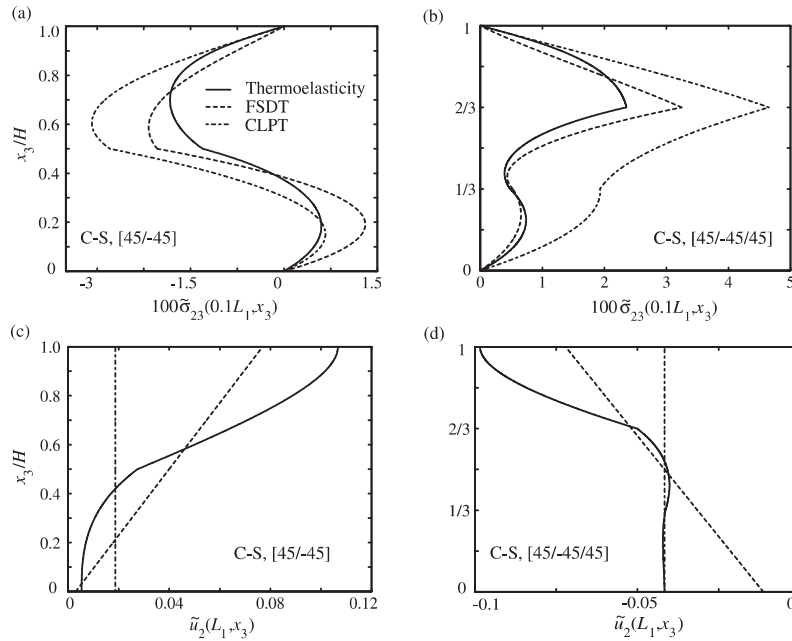


Fig. 8. The through-the-thickness distribution of (a, b) the nondimensional transverse shear stress σ_{23} and (c, d) displacement u_2 for 2-layer and 3-layer angle-ply laminates, $L_1/H = 5$, and a thermal load applied on the top surface.

Table 3

Displacement and stresses at specific locations for 2-ply laminates subjected to various boundary conditions, $L_1/H = 5$. A thermal load is applied to the top surface of the laminate

Variable	[0/90]			[90/0]			[45/-45]		
	S-S	C-F	C-S	S-S	C-F	C-S	S-S	C-F	C-S
$10\tilde{u}_1(L_1/4, H)$	-10.495	2.880	-4.203	-1.642	0.483	-0.125	-5.654	1.702	-1.601
$10\tilde{u}_2(3L_1/4, H)$	0.000	0.000	0.000	0.000	0.000	0.000	1.734	3.535	0.551
$\tilde{u}_3(L_1/2, H/2)$	2.603	-1.528	1.179	0.502	-0.332	0.213	1.657	-1.000	0.717
$10\tilde{\sigma}_{11}(L_1/2, H)$	-2.805	-2.818	-4.441	-4.531	-4.559	-5.910	-2.906	-2.913	-4.723
$10\tilde{\sigma}_{11}(L_1/2, 0)$	-9.171	-9.302	-2.414	-0.278	-0.278	0.044	-2.049	-2.042	-0.232
$10\tilde{\sigma}_{13}(L_1/4, H/4)$	0.400	0.308	0.702	0.032	0.020	0.046	0.098	0.086	0.204
$10\tilde{\sigma}_{23}(L_1/4, 3H/4)$	0.000	0.000	0.000	0.000	0.000	0.000	-0.144	-0.125	-0.168
$100\tilde{\sigma}_{33}(L_1/2, 3H/4)$	0.289	0.278	0.276	0.175	0.168	0.166	0.148	0.148	0.147

surface $x_1 = L_1$. The corresponding transverse shear stress on the midplane of clamped simply supported laminates is given in Fig. 7(c) and (d). In this case too, the oscillations are present at points on the interface between the adjoining laminae that are near the clamped edge. Fig. 8(a) and (b) depict the through-the-thickness distribution of the transverse shear stress σ_{23} for antisymmetric and symmetric angle-ply C-S laminates. The corresponding plots of the displacement u_2 are given in Fig. 8(c) and (d). The thermoelasticity solution exhibits a highly nonlinear through-the-thickness behavior for u_2 . The predictions from the CLPT and the FSDT that can at best represent an affine behavior for u_2 are in considerable error. Numerical results for 2-ply and 3-ply laminates subjected to various boundary conditions are given in Tables 3 and 4. They can be used to compare predictions from various plate theories and finite-element solutions.

Table 4

Displacement and stresses at specific locations for 3-ply laminates subjected to various boundary conditions, $L_1/H = 5$. A thermal load is applied to the top surface of the laminate

Variable	[0/90/0]			[90/0/90]			[45/−45/45]		
	S-S	C-F	C-S	S-S	C-F	C-S	S-S	C-F	C-S
$10\tilde{u}_1(L_1/4, H)$	−1.743	0.512	−0.168	−8.243	2.221	−3.211	−4.567	1.063	−1.128
$10\tilde{u}_2(3L_1/4, H)$	0.000	0.000	0.000	0.000	0.000	0.000	−0.700	−0.912	−0.696
$\tilde{u}_3(L_1/2, H/2)$	0.405	−0.247	0.217	2.723	−1.583	1.177	1.219	−0.596	0.607
$10\tilde{\sigma}_{11}(L_1/2, H)$	−4.083	−4.100	−5.502	−3.812	−3.821	−5.058	−3.505	−3.519	−5.051
$10\tilde{\sigma}_{11}(L_1/2, 0)$	−0.795	−0.790	0.618	−1.924	−1.921	−0.687	−1.631	−1.621	−0.088
$100\tilde{\sigma}_{13}(L_1/4, H/2)$	0.134	0.073	1.247	1.863	1.744	4.219	0.268	0.278	1.814
$100\tilde{\sigma}_{23}(L_1/4, H/2)$	0.000	0.000	0.000	0.000	0.000	0.000	1.112	0.721	1.287
$1000\tilde{\sigma}_{33}(L_1/2, H/2)$	0.279	0.239	0.231	6.763	6.664	6.624	2.913	2.894	2.882

6. Conclusions

We have used the Eshelby–Stroh formalism to study the generalized plane strain thermoelastic deformations of anisotropic thick laminated plates subjected to arbitrary mechanical and thermal boundary conditions at the edges. The three-dimensional equations of quasi-static, linear, anisotropic thermoelasticity simplified to the case of generalized plane strain deformations are exactly satisfied at every point in the body. The analytical solution is in terms of an infinite series; the continuity conditions at the interfaces and boundary conditions on the bounding surfaces are used to determine the coefficients.

Results for a thermal load applied on the top surface are presented for antisymmetric and symmetric cross-ply and angle-ply laminated plates with clamped, traction-free or simply supported edges. Our computed results for simply supported plates agree with those of Tauchert. The thermoelasticity results are compared with the predictions of the classical laminated plate theory and the first-order shear deformation theory. The thermoelasticity solution depicts a quadratic through-thickness variation of the transverse displacement. For a single layer 0° homogeneous cantilever laminate of thickness $0.2L_1$, the longitudinal distribution of the transverse shear stress exhibits boundary layers of width $0.25L_1$ and $0.08L_1$ at the clamped and traction-free edges, respectively, where L_1 equals the span of the plate. We note that the width of the boundary layer will generally decrease with an increase in the value of L_1/H . The transverse shear and transverse normal stresses computed from the CLPT and the FSDT exhibit significant errors near the clamped and traction-free edges where the influence of the boundary layer is significant. The CLPT and the FSDT give good results for the longitudinal stress. In the case of angle-ply laminates, the FSDT and the CLPT are not able to capture the complicated through-thickness behavior of the displacement u_2 .

The computed results prove the versatility of the proposed technique for obtaining accurate stresses for thick laminates subjected to various boundary conditions. The tabulated results presented herein should help establish the validity of various plate theories.

Acknowledgements

This work was partially supported by the NSF grant CMS9713453 and the ARO grant DAAG55-98-1-0030 to Virginia Polytechnic Institute and State University. R.C. Batra was also supported by an Alexander von Humboldt Award.

References

- Ali, J.S.M., Bhaskar, K., Varadan, T.K., 1999. A new theory for accurate thermal/mechanical flexural analysis of symmetric laminated plates. *Composite Structures* 45, 227–232.
- Carlson, D.E., 1972. *Linear thermoelasticity*. Handbuch der Physik, VIa/2, Springer, Berlin.
- Cho, K.N., Striz, A.G., Bert, C.W., 1989. Thermal stress analysis of laminate using higher-order theory in each layer. *Journal of Thermal Stresses* 12, 321–332.
- Clements, D.L., 1973. Thermal stress in anisotropic elastic half-space. *SIAM Journal of Applied Mathematics* 24, 332–337.
- Dempsey, J.P., Sinclair, G.B., 1979. On the stress singularities in the plane elasticity of the composite wedge. *Journal of Elasticity* 9, 373–391.
- Eshelby, J.D., Read, W.T., Shockley, W., 1953. Anisotropic elasticity with applications to dislocation theory. *Acta Metallurgica* 1, 251–259.
- Hwu, C., 1990. Thermal stresses in an anisotropic plate disturbed by an insulated elliptic hole or crack. *Journal of Applied Mechanics* 57, 916–922.
- Jones, R.M., 1975. *Mechanics of Composite Materials*. Scripta Book Co., Washington, D.C.
- Khdeir, A.A., Reddy, J.N., 1991. Thermal stresses and deflections of cross-ply laminated plates using refined plate theories. *Journal of Thermal Stresses* 14, 419–438.
- Khdeir, A.A., Reddy, J.N., 1999. Jordan canonical form solution for thermally induced deformations of cross-ply laminated composite beams. *Journal of Thermal Stresses* 22, 331–346.
- Mathieu, E., 1890. *Théorie de l'élasticité des corps solides, seconde partie*, Gauthier-Villars, Paris, pp. 140–178 (Chapter 10).
- Murakami, H., 1993. Assessment of plate theories for treating the thermomechanical response of layered plates. *Composites Engineering* 3, 137–149.
- Noor, A.K., Burton, W.S., 1992. Computational models for high-temperature multilayered composite plates and shells. *Applied Mechanics Reviews* 45, 419–446.
- Noor, A.K., Kim, Y.H., Peters, J.M., 1994. Transverse shear stresses and their sensitivity coefficients in multilayered composite panels. *AIAA Journal* 32, 1259–1269.
- Pagano, N.J., 1970. Influence of shear coupling in cylindrical bending of anisotropic laminates. *Journal of Composite Materials* 4, 330–343.
- Pell, W.H., 1946. Thermal deflections of anisotropic thin plates. *Quarterly of Applied Mathematics* 4, 27–44.
- Reddy, J.N., 1997. *Mechanics of Laminated Composite Plates: Theory and Analysis*. CRC Press, Boca Raton, FL.
- Reddy, J.N., Bert, C.W., Hsu, Y.S., Reddy, V.S., 1980. Thermal bending of thick rectangular plates of bimodulus composite materials. *Journal of Mechanical Engineering Science* 22, 297–304.
- Reddy, J.N., Hsu, Y.S., 1980. Effects of shear deformation and anisotropy on the thermal bending of layered composite plates. *Journal of Thermal Stresses* 3, 475–493.
- Savoia, M., Reddy, J.N., 1995. Three-dimensional thermal analysis of laminated composite plates. *International Journal of Solids and Structures* 32, 593–608.
- Savoia, M., Reddy, J.N., 1997. Three-dimensional thermal analysis of laminated composite plates-closure. *International Journal of Solids and Structures* 34, 4653–4654.
- Srinivas, S., Rao, A.K., 1972. A note on flexure of thick rectangular plates and laminates with variation of temperature across thickness. *Bulletin of the Polish Academy of Sciences, Technical Sciences* 20, 229–234.
- Stavsky, Y., 1963. Thermoelasticity of heterogeneous anisotropic plates. *Journal of Engineering Mechanics Division, Proceedings of ASCE* 89, 89–105.
- Stroh, A.N., 1958. Dislocations and cracks in anisotropic elasticity. *Philosophical Magazine* 3, 625–646.
- Tauchert, T.R., 1980. Thermoelastic analysis of laminated orthotropic slabs. *Journal of Thermal Stresses* 3, 117–132.
- Tauchert, T.R., 1991. Thermally induced flexure, buckling, and vibration of plates. *Applied Mechanics Reviews* 44, 347–360.
- Thangjitham, S., Choi, H.J., 1991. Thermal stresses in a multilayered anisotropic medium. *Journal of Applied Mechanics* 58, 1021–1027.
- Ting, T.C.T., 1996. *Anisotropic Elasticity. Theory and Applications*. Oxford Engineering Science Series, No 45. Oxford University Press, New York.
- Ting, T.C.T., Hwu, C. 1991. Effects of heat flow on stress singularities at the interface crack. In: Singhal, S.N., Jones, W.F., Herakovich, C.T. (Eds.), *Mechanics of Composites at Elevated and Cryogenic Temperatures*, AMD-vol. 118. ASME, pp. 231–238.
- Tungikar, V.B., Rao, K.M., 1994. Three dimensional exact solution of thermal stresses in rectangular composite laminate. *Composite Structures* 27, 419–430.
- Vel, S.S., Batra, R.C., 1999. Analytical solution for rectangular thick laminated plates subjected to arbitrary boundary conditions. *AIAA Journal* 37, 1464–1473.
- Vel, S.S., Batra, R.C., 2000. The generalized plane strain deformations of anisotropic composite laminated thick plates. *International Journal of Solids and Structures* 37, 715–733.

- Whitney, J.M., Pagano, N.J., 1970. Shear deformation in heterogeneous anisotropic plates. *Journal of Applied Mechanics* 37, 1031–1036.
- Wu, C.H., 1984. Plane anisotropic thermoelasticity. *Journal of Applied Mechanics* 51, 724–726.
- Wu, C.H., Tauchert, T.R., 1980a. Thermoelastic analysis of laminated plates 1: symmetric specially orthotropic laminates. *Journal of Thermal Stresses* 3, 247–259.
- Wu, C.H., Tauchert, T.R., 1980b. Thermoelastic analysis of laminated plates 2: antisymmetric cross-ply and angle-ply laminates. *Journal of Thermal Stresses* 3, 365–378.
- Yang, P.C., Norris, C.H., Stavsky, Y., 1966. Elastic wave propagation in heterogeneous plates. *International Journal of Solids and Structures* 2, 665–684.
- Yang, X.X., Shen, S., Kuang, Z.B., 1997. The degenerate solution for piezothermoelastic materials. *European Journal of Mechanics A Solids* 16, 779–793.